POLITECNICO DI TORINO
Repository ISTITUZIONALE

Highly-filled flowable composite in deep margin elevation: FEA study obtained from a microCT real model

Original
Highly-filled flowable composite in deep margin elevation: FEA study obtained from a microCT real model / Baldi, A., Scattina, A., Ferrero, G., Comba, A., Alovisi, M., Pasqualini, D., Peroni, L., Muggeo, M., Germanetti, F., Scotti, N.. - In: DENTAL MATERIALS. - ISSN 0109-5641. - ELETTRONICO. - 38:4(2022), pp. 94-107. [10.1016/j.dental.2021.10.005]

Availability:
This version is available at: 11583/2973406 since: 2025-02-17T09:07:15Z

Publisher:
Elsevier

Published
DOI:10.1016/j.dental.2021.10.005

Terms of use:

This article is made available under terms and conditions as specified in the corresponding bibliographic description in the repository

Publisher copyright
Elsevier postprint/Author's Accepted Manuscript

© 2022. This manuscript version is made available under the CC-BY-NC-ND 4.0 license
http://creativecommons.org/licenses/by-nc-nd/4.0/.The final authenticated version is available online at:
http://dx.doi.org/10.1016/j.dental.2021.10.005

(Article begins on next page)

21 November 2026

Highly-filled flowable composite in deep margin elevation: FEA study obtained from a microCT real model.

1. INTRODUCTION

Carious class II cavities with iuxtagingival and subgingival margins in posterior teeth represent a daily challenge for clinicians. These interproximal lesions present technical difficulties mainly related to rubber dam isolation and cervical margin finishing procedures [1]. The subgingival extension also poses problems on adhesive procedures, since little or no enamel is usually available in the cervical area. It is globally accepted that adhesion is stable and efficient on enamel [2], while on dentin it is less reliable due to substrate morphology [3], being also influenced by the adhesive type [4] and the application technique [5]. Another aspect that must be considered is that thermo-mechanical load conditions could cause premature bond degradation in this critical area, ultimately leading to restoration failure [6,7].

In order to avoid periodontal surgery when the biological width is maintained [8], the cervical margin relocation procedure, subsequently renamed "Deep margin elevation", has been proposed [9,10]. Different materials have been used for this technique and two main protocols have been proposed. The open-sandwich protocol consists in placing a first horizontal layer of resin-modified glass-ionomer or, more recently, of flowable resin composite on the cervical margin, then finalize the restoration with a conventional material [11]. The closed-sandwich protocol, on the other hand, consists in placing the composite or, eventually, a ceramic inlay immediately, as unique material [11]. Flowable composite application in the open-sandwich protocol is based on the rational that a flowable material should be easier to manipulate and adapt to the deep cavity floor than the glass-ionomer [12,13]. Moreover, the lower elasticity modulus of flowable resins has been reported to potentially decrease shrinkage stress and the consequent interfacial gap formation during polymerization [14]. This might help reducing postoperative sensitivity, secondary caries and periodontal problems [15,16]. From a mechanical point of view, another aspect that has been recently highlighted is that an open-sandwich protocol might decrease ceramic fracture when preparation margins are located below CEJ [17]. However, there is no consensus about the influence of deep margin elevation technique on fracture strength of different adhesive restorations [18,19]. Flowable materials present lower mechanical properties compared to traditional composites, due to the lower percentage of filler load [12], and it has been recently suggested that this might lead to premature adhesive failure when cyclic loads are applied [20]. In order to merge the best proprieties of flowable and conventional resin composites, highly-filled flowable composites have been recently introduced [21]. These composites

take advantage of new monomers, that contribute to maintain flowability even if highly-loaded with fillers, ultimately improving mechanical performance [22].

Nowadays, materials are in constant evolution, so it is difficult to test and compare their performances. In this sense, Finite Elements Method (FEM) is useful to perform fast, predictable investigations comparing different materials in the exact same conditions, without the need of prototyping [23]. FEM consists in discretizing the 3D geometry of the tooth with small elements, calculating load conditions and deformation state for each one and then assembling the results for the whole structure. FEM has been validated by several studies [24], that measured shrinkage forces and residual stresses of different restorative materials [25,26]. However, most of the FEM studies are based on CAD-generated restorations and focus on the material behavior itself rather than working on realistic restorations and analyzing their interfacial behavior.

To the best of our knowledge there is no consensus about which materials and techniques should be used in deep margin elevation to achieve the best interfacial performances. Moreover, there is a lack of data regarding highly-loaded flowable composites applied to deep margin elevation and their behavior under load. Thus, the aim of the present study was to evaluate, through FEM analysis focusing on shear stress (SS) and normal pressure (NP) consequent to axial load, the interfacial behavior of a new highly-loaded flowable composite, applied with different techniques and materials, to a deep margin elevation scenario.

The null hypotheses tested were that the interfacial load conditions are not influenced by (1) the occlusal restorative material, (2) the usage of a highly-filled flowable composite as liner and (3) the substrate of the cervical margins.

2. MATERIALS AND METHODS

2.1 Specimen preparation

A single intact human upper molar, extracted for periodontal reasons within the last month, was selected and stored in distilled water after disinfection with an ultrasonic device. The study was granted ethics approval by the local ethics committee of the Dental School, University of XXX (DS-2018_No.001). The selected tooth was examined and confirmed to be sound, with no carious lesions, demineralization, cracks, or signs of wear under 20x magnification optical microscope.

Two standardized class II cavities, one mesial and one distal, were created on the specimen by the same expert operator with the following dimensions: 4 mm in the buccal–oral direction and 3 mm in the mesio-distal direction. The mesial cavity cervical margin was set 1 mm above the CEJ, whereas the distal cervical margin was set 1 mm below the CEJ.

A circumferential steel matrix was applied (Automatrix; Dentsply, Konstanz, Germany) and tightened until a perfect fit with the cervical margins was achieved. Then, the specimen was subjected

to the adhesive procedure: selective enamel etching for 30 s with 35% phosphoric acid (K-etchant, Kuraray Noritake Dental, Mie, Japan), rinsing for 30 s, and air-drying. A two-step self-etch adhesive system (Clearfil SE Bond2; Kuraray Noritake Dental, Mie, Japan) was then applied following the manufacturer's instructions, and slightly air-dried before light-curing for 40 s with a light-emitting diode (LED) lamp at 1400 mW/cm^2 (Cefalux2; Voco, Cuxhaven, Germany). Then, 2 mm standardized composite layers were applied progressively (Filtek Supreme XTE; 3M ESPE, St Paul, MN, USA), each being light-cured with the same LED lamp for 20 s. Finishing and polishing procedures were then performed with abrasive disks (SofLex; 3M ESPE, St Paul, MN, USA) and silicon points (Enhance; Dentsply, Konstanz, Germany). The final restorations were confirmed to be clinically acceptable by an expert operator. An overview of the simulated restorative materials, their manufacturers, classification and composition are reported in Table 1.

Material	Manufacturer	Classification	Composition
e.max CAD	Ivoclar Vivadent, Schaan, Lichtenstein	Lithium disilicate	SiO2, Li2O, K2O, P2O5, ZrO2, ZnO, Al2O3, MgO
Filtek Supreme XTE	3M ESPE, St. Paul, MN, USA	Nano-filled resin composite	Organic part: Bis-GMA, Bis-EMA, PEGDMA, TEGDMA Fillers (65 wt% = 46 vol%): ytterbium trifluoride (0.1-5 lm), nonagglomerated/nonaggregated surface modified 20-nm and 75-nm silica fillers, surface modified aggregated zirconia/silica fillers (cluster average size: 0.6-10 lm)
Majesty ES Flow Super low	Kuraray Noritake Dental, Tokyo, Japan	Highly-filled flowable resin composite	Organic part: TEGDMA, hydrophobic-aromatic dimethacrylate, dl-CQ, PI Fillers (78 wt% = 64 vol%): Barium glass filler, silica filler

Table 1. Simulated materials of the present study, alongside with their respective manufacturer, classification and composition.

2.2 Micro-CT reconstruction

A Micro-CT scan (SkyScan 1172; Bruker, Billerica, MA, USA) was employed to recreate an accurate 3D model of the tooth structure and the restorations. High-resolution scan was performed using the following parameters: voltage = 100 kV; current = 100 µA; aluminum and copper (Al+Cu) filter; pixel size = 20,27 µm; averaging = 5; rotation step = 0.6°. NRecon software (Bruker, Billerica, MA, USA) was used to reconstruct the images and obtain DCM files (DICOM, Digital Imaging and

Communications in Medicine) applying the following corrections: beam hardening = 15%, smoothing = 4, smoothing kernel = 2 gaussian, ring artifact correction = 7.

The obtained files were imported into a segmentation software (Mimics Medical ver. 20.0; Materialise, Ann Arbor, MI, USA). Thanks to the different radiodensity among structures, it was possible to automatically create multiple segments made up of pixel sets representative of enamel, dentin and restorative material. In order to ensure proper contacts between different masks, morphology operations, alongside with region growing algorithm and boolean operations were used. The final parts were then converted into optimal-quality STL files (STereo Lithography interface format), with a sample ratio 1:1.

A graphical workflow of the performed steps is reported in Figure 1.

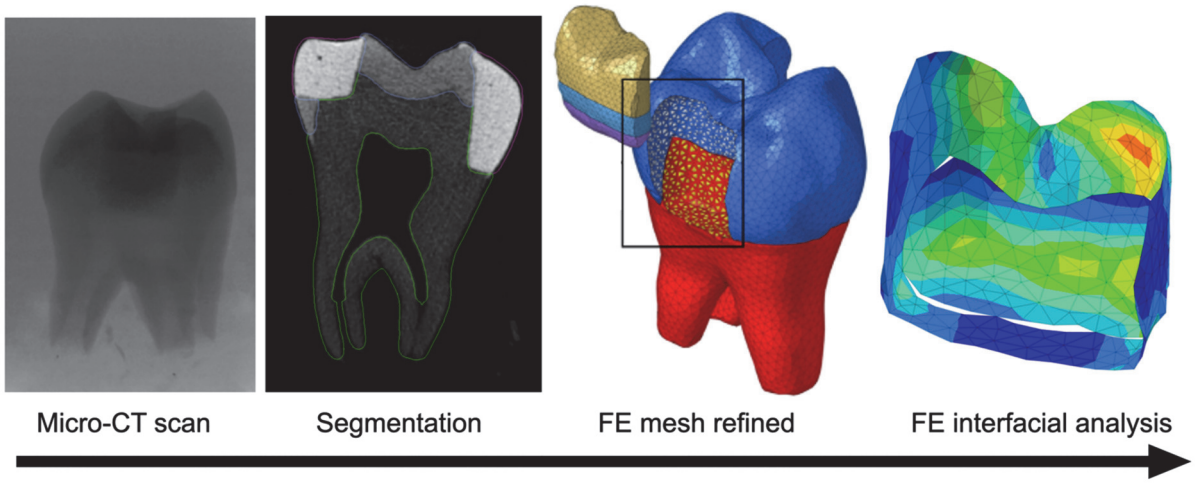


Figure 1. Summary of the performed steps from micro-CT to FE analysis. A maxillary molar was restored with two class II cavities and scanned with micro-CT. Segmentation allowed to create different meshes for dentin (red volume), enamel (blue volume) and restorations (separate volume consisting of different layers). Finite Element analysis was performed focusing on the interfacial behavior of the restorative materials tested.

2.3 FE model preparation

The obtained STL files were imported into Meshlab (ISTI, CNR, Pisa, Italy) in order to perform a refinement process. The process consisted in the decimation of the FEs and in the elimination of the degenerated elements. Moreover, holes on the geometry were filled and the normal of the elements were reoriented in the same direction for all the elements making the mesh suitable for volume elements generation. The two-dimensional model was successively converted into a tetrahedral mesh using Altair Hyperworks (Altair Engineering, Troy, Michigan, USA). Subsequently, in order to virtually reproduce the loading cycle of a chewing simulator machine, the sphere used in the experimental test to apply the load was discretized using shell elements with rigid material and the tooth was positioned within a resin disk, as shown in Figure 2. The total number of elements of the FE model, including resin disk and sphere, was approximately 135.000.

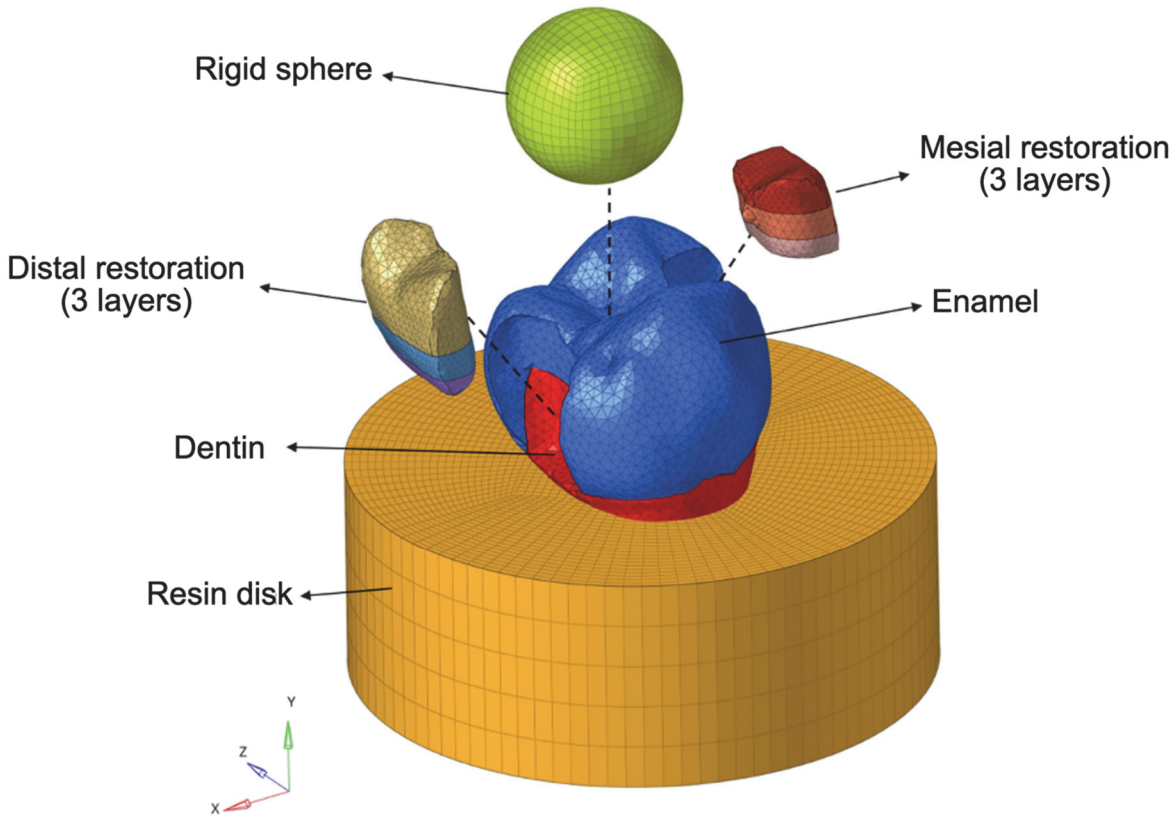


Figure 2. Representation of the simulated FE model. Each volume is reported alongside its description, as follows: green = rigid chewing sphere, blue = enamel, red = dentin, orange = resin disk. Mesial and distal restorations were divided into three segments in order to simulate different models, as explained in the text.

Restorations were segmented in three parts, in order to simulate a total of six different models (Figure 3), using different restorative materials and techniques as follows:

Model A: the entire restoration was simulated with lithium disilicate (IPS e.max CAD MT, Ivoclar Vivadent, Schaan, Liechtenstein);

Model B: the entire restoration was simulated with nano-filled conventional packable composite (Filtek Supreme XTE, 3M ESPE, St. Paul, MN, USA);

Model C: a 1.5 mm thick horizontal layer of highly-filled flowable resin composite (Majesty ES Flow super low, Kuraray Noritake Dental, Tokyo, Japan) was simulated as a first layer, over the cervical margin; the remaining restoration was simulated with nano-filled traditional composite (Filtek Supreme XTE, 3M ESPE, St. Paul, MN, USA);

Model D: same scenario of model B, but with 3 mm of highly-filled flowable composite (Majesty ES Flow super low, Kuraray Noritake Dental, Tokyo, Japan).

Model E: same as scenario C, using lithium disilicate (IPS e.max CAD MT, Ivoclar Vivadent, Schaan, Liechtenstein) instead of the nano-filled traditional composite

Model F: same as scenario E, but with 3 mm of highly-filled flowable composite (Majesty ES Flow super low, Kuraray Noritake Dental, Tokyo, Japan).

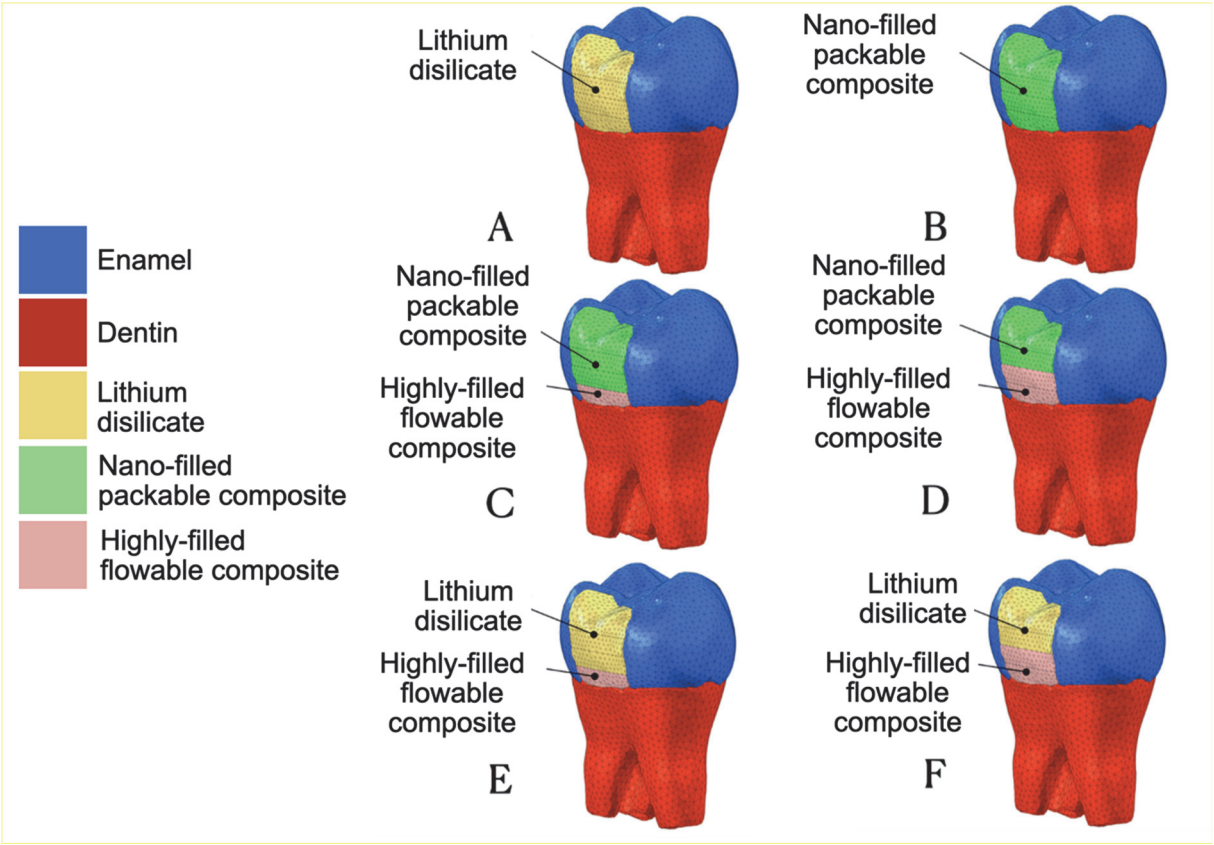


Figure 3. Schematic representation of the six simulated FE models. Materials are represented as follows: red = dentin, blue = enamel, yellow = lithium disilicate, green = nano-filled conventional packable composite and pink = highly-filled flowable resin composite.

Dentin, enamel and restorations were modelled with a linear elastic material model, whereas the resin disk and the chewing sphere were modelled as rigid materials, because the deformation of these parts is negligible compared to the other parts of the model subjected to load. Sphere-tooth contact was considered with an automatic surface-to-surface contact algorithm (Fig.4).

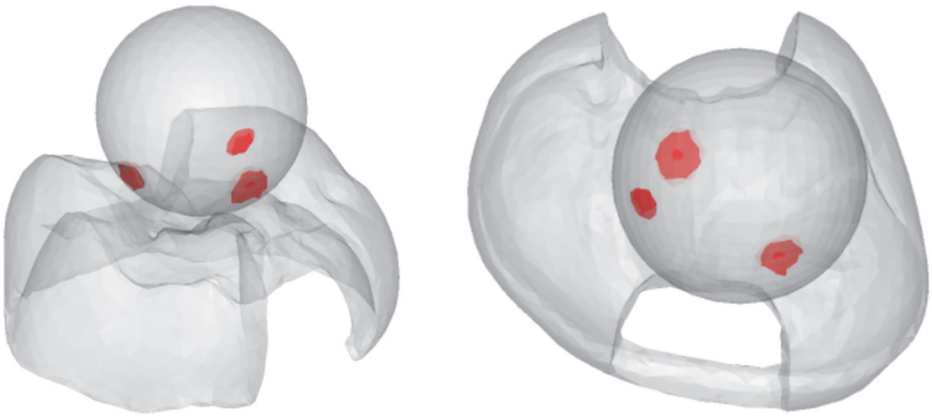


Figure 4. Contact points (red area) determined with a surface-to-surface contact algorithm.

The FE simulation was performed using LS-Dyna code in its explicit formulation. In order to reach the load applied during the experimental test, the simulation was set-up in the following way. Considering the explicit method, to increase the stability of the simulation, a motion law was applied to the sphere. In particular, a constant velocity in the vertical direction (Y axis in negative direction, referring to Figure 2), was applied to the sphere up to the applied load reached a value of 50 N.

The contact between the sphere and the tooth was set as a penalty-based formulation, whereas the joining between the other parts (enamel, dentin and restorations) were defined with a tied contact formulation with offset option, according to software house indications.

The load was aimed to simulate a single load cycle. Normal pressure and shear stress at the tooth-restoration interface were recorded (Figure 5).

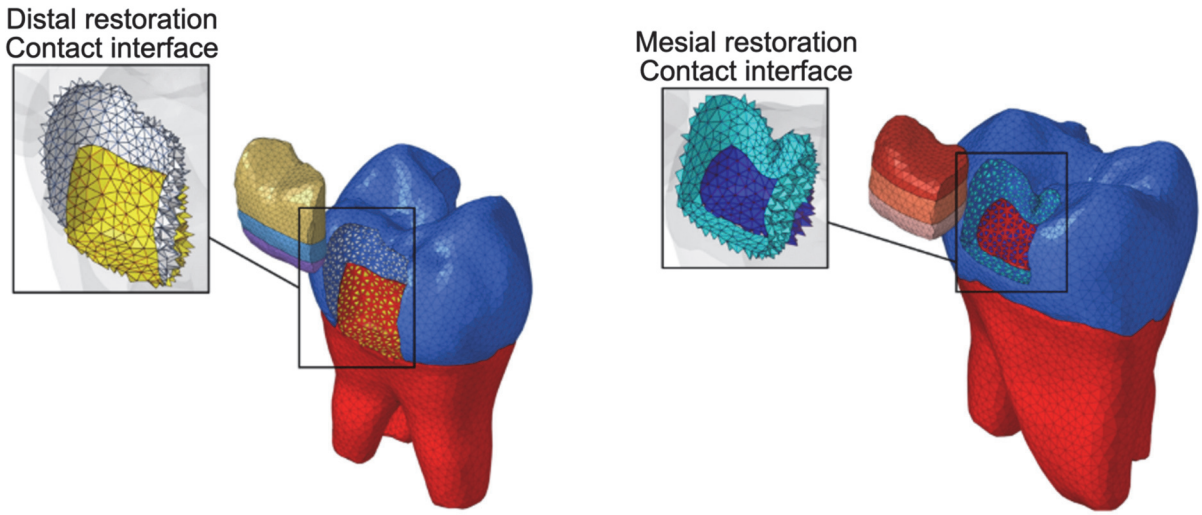


Figure 5. Highlights of the elements at the tooth-restoration interfaces of which normal pressure and shear stresses were evaluated. Left picture present a highlight of the distal restoration, while right picture of the mesial one.

Table 2 reports a summary of the mechanical characteristics given to the simulated materials, which were taken from the literature [27,28] or directly provided from the manufacturers. Table 3 reports a summary of volumes, expressed as mm^3, and elements, expressed as n°, for the different parts in different scenarios.

Material	**Young's modulus (GPa)**	**Poisson ratio**	**Density (g/cm^3)**
Enamel	78	0.33	3
Dentin	18	0.23	2.2
Allumina sphere	80	0.23	2.7

Resin Disk	3.5	0.33	1.54
Lithium disilicate (e.max CAD)	95	0.23	2.5
Nano-filled packable composite (Filtek Supreme XTE)	12.7	0.35	1.9
Highly-filled flowable composite (Majesty ES Flow Super low)	6.7	0.33	1.85

Table 2. Material properties of the FE parts, obtained from literature or provided from the manufacturers.

			SPHERE	RESIN DISC	ENAMEL	DENTIN	DISTAL	MESIAL		
Scenario A,B	volume	mm^3	111.62	1685.30	158.23	238.69	32.24	25.18		
	elements	n°	7000	3280	15638	24057	14834	13206		
							DISTAL		**MESIAL**	
			SPHERE	**RESIN DISC**	**ENAMEL**	**DENTIN**	**Lithium disilicate/Nano-filled packable composite**	**Highly-filled flowable composite**	**Lithium disilicate/Nano-filled packable composite**	**Highly-filled flowable composite**
Scenario C, E	volume	mm^3	111.62	1685.30	158.23	238.69	26.99	5.25	17.26	7.92
	elements	n°	7000	3280	15638	24057	11700	3134	9080	4126
							DISTAL		**MESIAL**	
			SPHERE	**RESIN DISC**	**ENAMEL**	**DENTIN**	**Lithium disilicate/Nano-filled packable composite**	**Highly-filled flowable composite**	**Lithium disilicate/Nano-filled packable composite**	**Highly-filled flowable composite**
Scenario D, F	volume	mm^3	111.62	1685.30	158.23	238.69	18.98	13.26	7.34	17.84
	elements	n°	7000	3280	15638	24057	7720	7114	3903	9303

Table 3. Number of elements and volume expressed in mm^3 for each single part in different tested scenario.

3. RESULTS

3.1 Normal pressure analysis

Figures 6a and 6b illustrate the contour maps of the normal pressure (at peak load) at the interface between the tooth and the restorations for the mesial cavity (enamel cervical margin) and the distal cavity (dentin cervical margin). All the pictures are representative of the tooth-restoration interfaces observed from outside the tooth, as previously shown in Figure 5. The results are presented with relative percentage values referred to model A to increase the comparability of the results between the different cases.

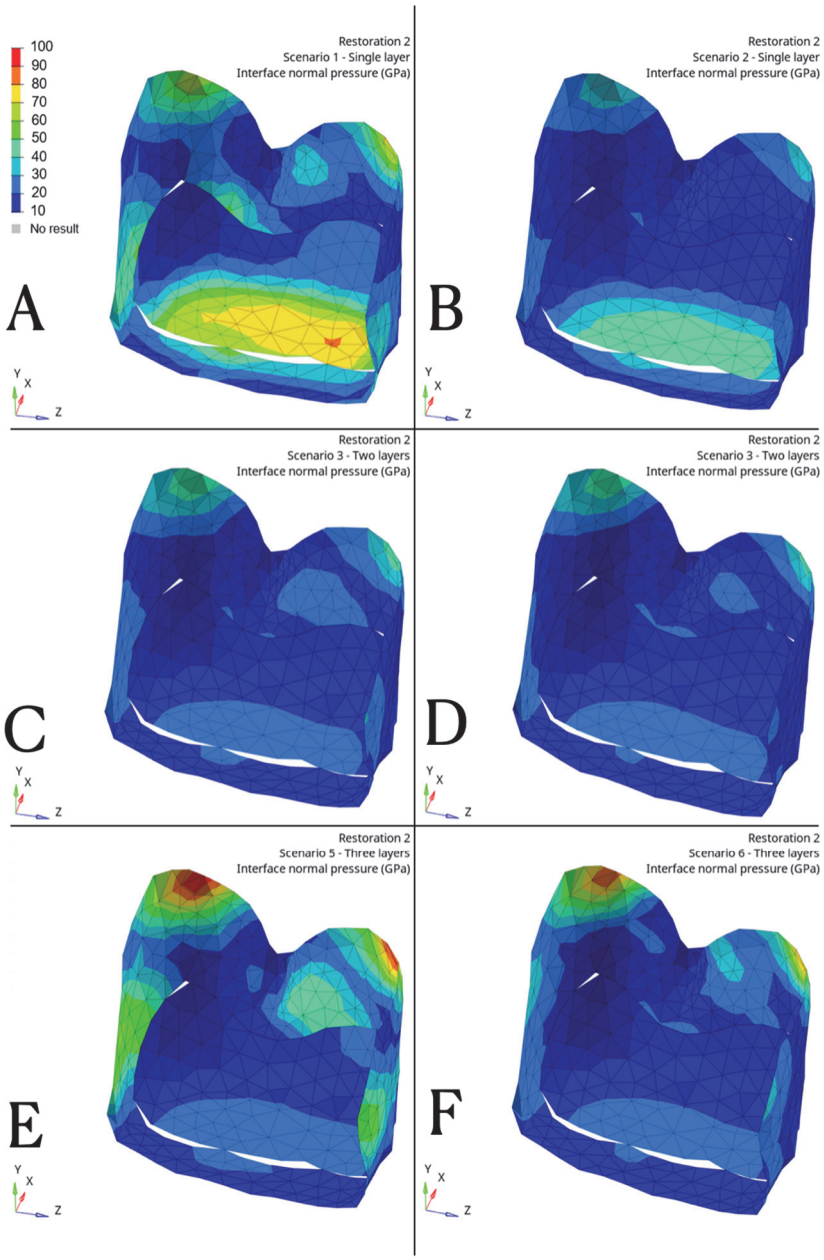


Fig.6a. Normal pressure distribution on the tooth-restoration interface, at the peak load, for the mesial cavity (enamel cervical margin). The legend reported to the left shows the maximum and the minimum values, respectively red and blue.

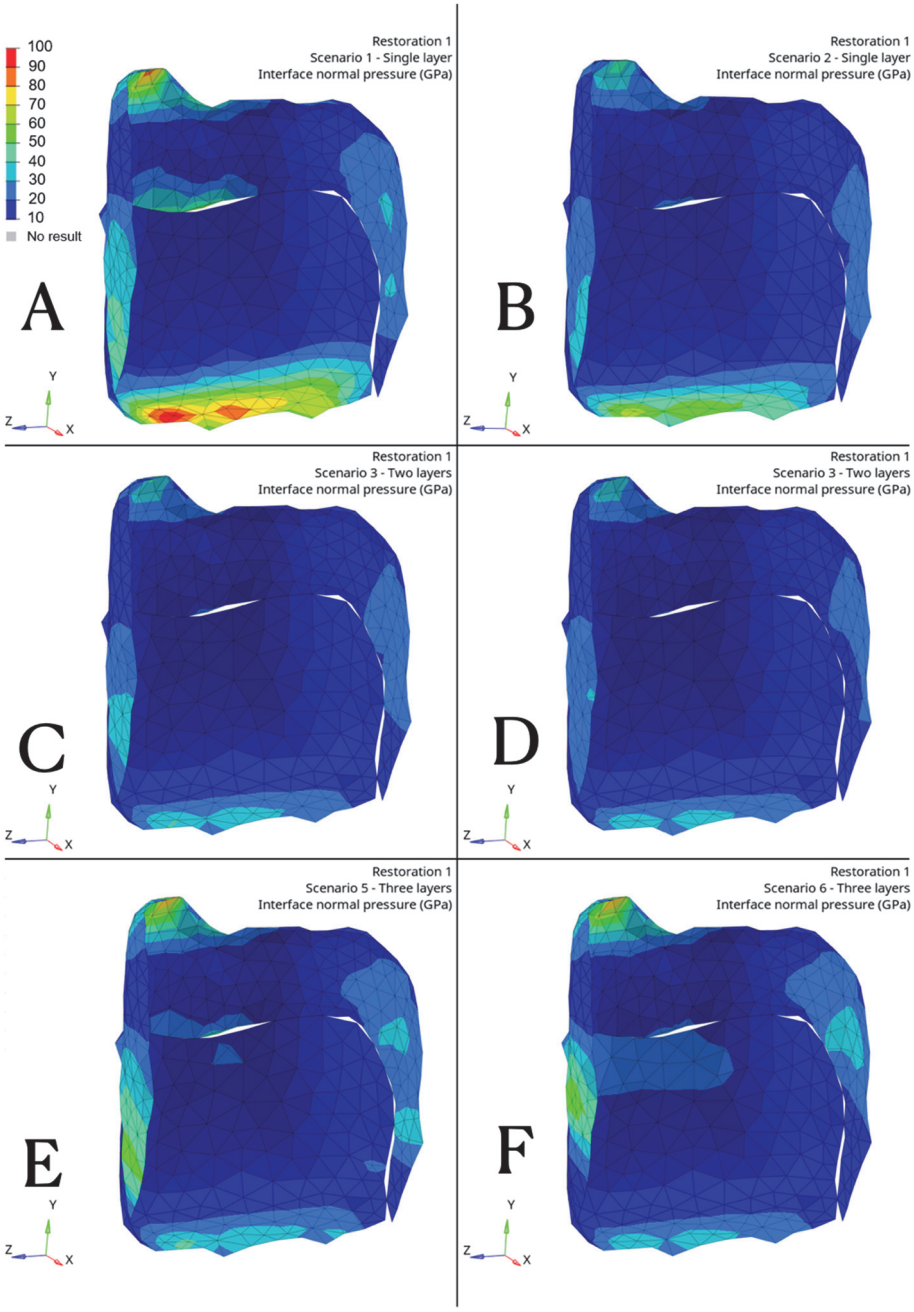


Fig.6b. Normal pressure distribution on the tooth-restoration interface, at the peak load, for the distal cavity (dentin cervical margin). The legend reported to the left shows maximum and minimum values, respectively red and blue.

For what concerns the mesial restoration (Fig. 56), the model that presented higher interfacial stresses is the model A. Most of the stresses appear to be concentrated on the inner cavity floor, while lower and not homogeneous stresses were found on the axial enamel and the cervical enamel margin. The model E presented ever higher interfacial stresses on the axial enamel, especially in the coronal part, but performed significantly better regarding the axial dentin, the cervical enamel margin and the cavity floor area compared to the model A. The model F showed a similar pressure distribution but it performed even better than the model E,

because the high stresses in the coronal enamel are reduced. The model B showed minor stresses on the cavity floor and the cervical enamel margin, with a homogeneous distribution among the whole surface in particular compared to the model A. The models C and D both performed significantly better than the others, appearing as equally the best solutions. It was also possible to observe that, in all the models, cervical enamel margin showed less stresses compared to the inner cavity floor, therefore probably acting as a force-breaker.

As regards to the distal restoration (Fig. 6b), the results confirmed the trend obtained on the mesial restoration. The model A showed the worst behavior, with high stresses on the cavity floor and a peak load in the cervical margin. Minor stresses were also reported among axial enamel, with a homogenous distribution. The models E and F showed again better results compared to the model A, except for the axial enamel stresses that increased and were localized more coronally. In this case, the model F is slightly worse than the model E because the pressure distributions are a little bit higher. The model B showed an overall good stress distribution, but the models C and D performed again significantly better in the cavity floor area.

3.2 Shear stress analysis

Figures 7a and 7b illustrate the contour maps of shear stresses (at peak load) at the interface between the tooth and the restoration for the mesial cavity (enamel cervical margin) and the distal cavity (dentin cervical margin). The results are presented with relative percentage values referred to model A in order to increase the comparability of the results between the different cases.

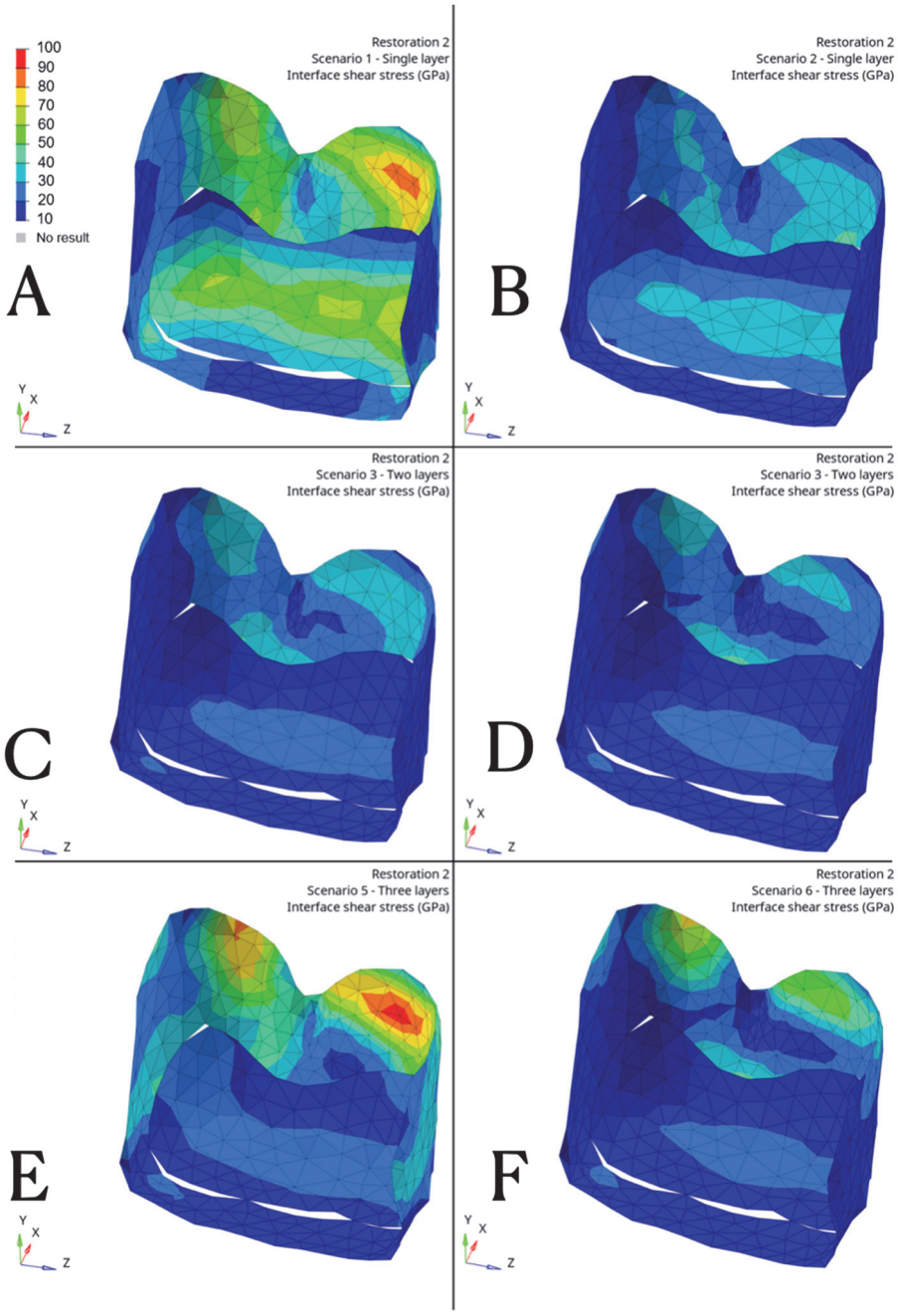


Fig.7a. Shear stress distribution on the tooth-restoration interface, at the peak load, for the mesial cavity (enamel cervical margin). The legend reported to the left shows the maximum and the minimum values, respectively red and blue.

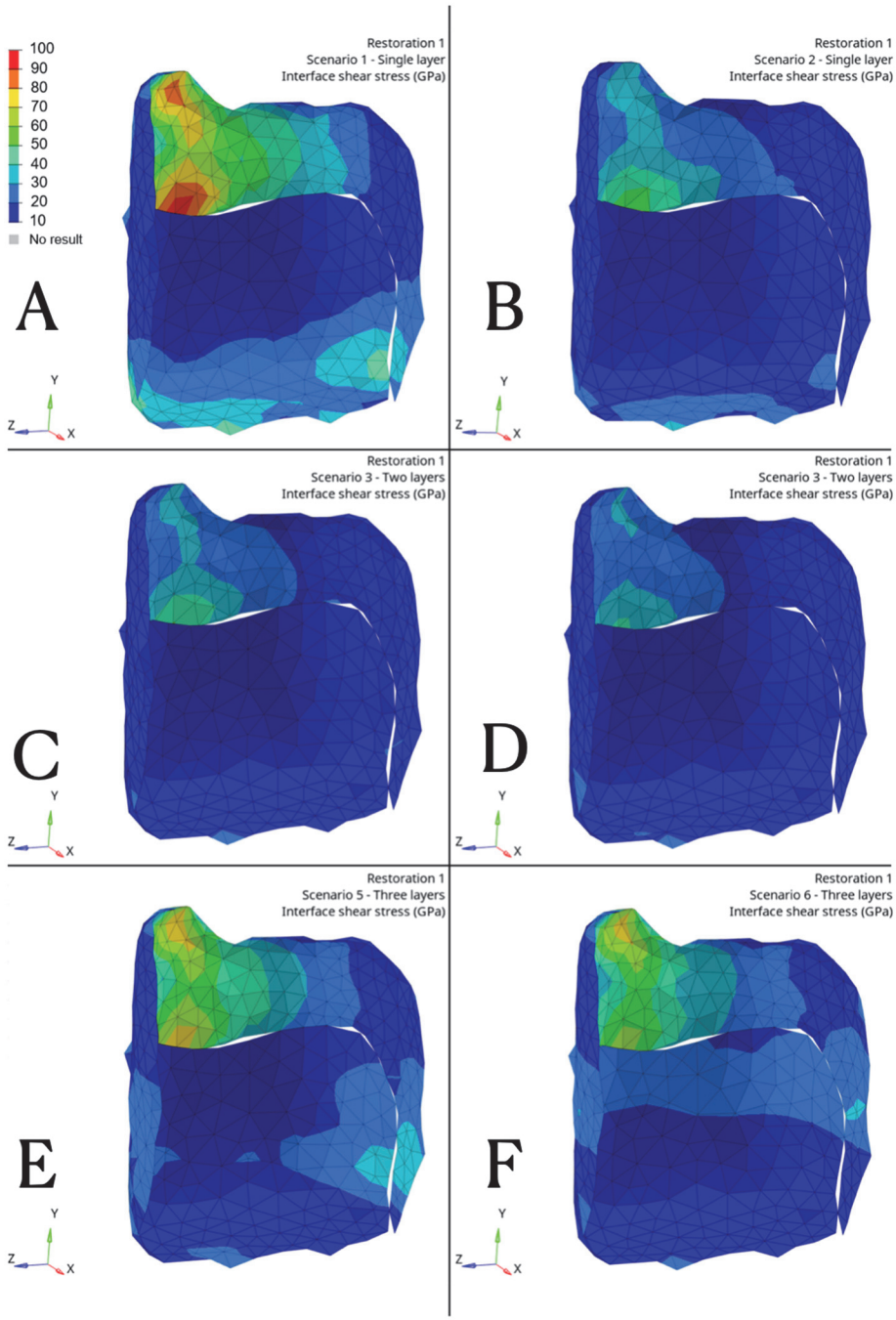


Fig.7b. Shear stress distribution on the tooth-restoration interface, at the peak load, for the distal cavity (dentin cervical margin). The legend reported to the left shows the maximum and the minimum values, respectively red and blue.

Regarding the mesial cavity (Fig. 7a), the model A showed the worst overall behavior, with high stresses on the cavity floor, the cervical and axial enamel margins. Alike to what previously reported in the normal pressure analysis, the models E and F performed significantly better than the model A, even if the model E showed higher stresses on axial enamel margins, because the stress distribution showed average lower values. The models B, C and D showed

low and well distributed stresses, with the models C and D performing slightly better than B on the cavity floor area.

As for the distal cavity (Fig. 7b), the model A showed the worst interfacial response, especially on the axial enamel and the cavity floor. The stress distribution showed the highest average stress values moreover with two important peaks. The model E performed significantly better than A, but few noticeable stresses persisted on the cavity floor area and the axial enamel. In this scenario, the model F worked slightly better than E, showing only low axial stresses in a very coronal position, with complete preservation of the cavity floor. Once more, the model B only showed few stresses in the coronal enamel and in the cavity floor. The models C and D had again the optimal performance, with minimum stresses only in the coronal enamel.

4. DISCUSSION

The present study analyzed the interfacial mechanical behavior of highly-filled flowable resin composite employed in deep margin elevation through FEM analysis. Based on the obtained results, all the three null hypotheses tested were rejected.

As regards the first null hypothesis, both tensile and shear stresses showed significant differences between tested occlusal materials. In particular, overall higher stresses were reported for lithium disilicate inlay compared to the nano-filled composite filling, both when they were employed alone (model A vs B) and when they were leaned on the highly-filled flowable composite (model C vs E and model D vs F). Being more specific, when the materials were employed alone (model A vs B), lithium disilicate presented higher shear stresses and normal pressure on axial walls, cavity floor and cervical margin. Contrastingly, when lithium disilicate was applied on the highly-filled flowable composite (models E and F), higher stresses were reported only on axial walls, in the closest area to the contact point of the load. This can be explained by the different mechanical properties of the materials, as ceramic has a higher Young's modulus [29], and therefore a stiffer behavior that creates higher stresses on the same deformation [30]. On the other hand, composite materials have a low Young's modulus because of the resin matrix [31], that might cause a more homogeneous distribution of the forces, as confirmed by the present study results [32]. When restoring multiple teeth or in case of hard-to-manage interproximal areas, even if the indirect solution with lithium disilicate could be less common than the direct composite approach, ceramic inlays clinically showed excellent mechanical proprieties and long-term performances, [33,34]. Moreover, as for direct restorations, ceramic inlays need adhesive cementation in order to increase over-time performances, therefore isolation must be considered a crucial factor [35]. As a consequence and accordingly to the present study results, in order to make isolation and cementation

procedures easier and to prevent stress concentration, deep margin elevation with highly-filled flowable resin composites could be successfully applied under ceramic inlays [36].

The second null hypothesis was also rejected, because the use of a highly-filled flowable composite as liner on the cervical margin significantly influenced the resulting shear and tensile stresses, with better performances (lower stresses and more uniform distribution) in the cavity floor and cervical margin areas whenever a deep margin elevation technique was applied (model A vs E-F and Model B vs C-D). This is in accordance with Ausiello *et al.* that already showed with FEM study how Young's modulus values of the restorative materials play an essential role in the stress distribution [37]. Other studies indirectly came to the same conclusions analyzing the interfacial behavior of flowable composite used as cavity liners, even if data cannot be compared directly to the present study due to different methodology and materials [38,39]. Data also showed a slight trend of developing inferior shear stresses and normal pressure when two layers of highly-filled flowable material were applied instead of a single layer (model C vs D and model E vs F). This trend is consistent with the previously reported discussion: the thicker the elastic layer, the higher the elastic deformation that can distribute stresses [28]. Given the present results, it is reasonable to assume that the highly-filled flowable composite could be useful to improve tensile and shear stresses distribution in the cervical area.

Lastly, the third null hypothesis was rejected, because a different stress distribution was observed in the cavity floor area according to the substrate (mesial vs distal cavities). In particular, enamel cervical margin seemed to play a protective role in the stress distribution, always showing inferior stress values compared to dentin cervical margin. This stress-breaker effect could be explained by the different mechanical proprieties of the dentin and enamel when related to the elasticity of the employed materials [40]. Dentin mechanical proprieties are more similar to that of composite compared to ceramics and this might lead to a more homogeneous distribution of forces. The exact opposite can be said for enamel and ceramic, that directly transmit forces to the adjacent structures [41]. As a consequence, the absence of cervical enamel should be considered a critical factor, not only from an adhesive point of view, but also biomechanically. Without cervical enamel a major attention should be given to the management of stresses in the cavity-base, since stresses will be more prone to concentrate in the outer interfacial area, leading to possible interfacial gap formation.

Another aspect to highlight is that the position of the loading point has a correspondence with the stress peaks distribution, as it has been shown in numerous other FEM studies [28,42]. Indeed, it can be observed that the contact points of the sphere determined the localization of the maximum stress area on the tooth-restoration interface in the nearest point in projection.

Even if the sphere tries to realistically replicate a conventional 3-contact point chewing, the stress peaks depend on the initial position of the sphere, and therefore the occlusal area with higher stress. As a consequence, cavity design and occlusal morphology will play a crucial role to avoid stress concentration. In accordance, it could be indirectly speculated that the occlusal contact points should not be placed on the tooth-restoration interface, but rather away from it, in order to avoid stress peaks along the adhesive interface.

For what concerns the methodology, FEM has already been proved to be an efficient and predictable method to simulate and analyze the mechanical behavior of dental materials [24]. Outdated FEM studies used 3D CAD models, with severe limitations in terms of realism [43]. More recently, 3D model reconstruction from micro-CT has been introduced, bringing to the creation of a more realistic virtual model [24,44]. However, most of the studies with micro-CT only segmented enamel and dentin, subsequently creating the restorations through CAD software, with limitations in terms of realism, especially in the corner area, since burs are not able to create perfect geometrical shapes [28,45]. In the present study, a healthy tooth was first cavitated and restored, then scanned and fully segmented aiming to better reproduce a clinical scenario [44]. Real restorations are not comparable to perfect shapes, indeed presenting voids, gaps and complex individual geometries which could have an impact on mechanical simulation and stress distribution. In previous works [28], FEM was used to study the global stress state in a restored tooth by means of linear analysis. In the present work non-linear analysis were carried out, allowing to obtain the complete stress state on the whole interface surfaces of a restored tooth. The stress state at the interface was studied considering both the shear stresses and the normal component (normal pressure). The analysis of these two entities allowed to understand how the tooth and the adhesive layer are stressed. These information are also useful to study potential long-term effects on the restoration.

A limitation of the FE models adopted in this work concerns the absence of the adhesive layer mesh. This might affect ceramic performances since it has been demonstrated that glass ceramics mechanical behavior benefit from adhesive cementation [46]. However, at the state of the art, it is quite difficult to get a realistic and precise micro-CT volume definition for the adhesive layer that could be easily translated in a FE model, due to its thickness and material properties [47,48]. Excluding the adhesive layer allows faster computation (both considering the pre-process and the solution time) and avoid introducing potential mistakes in this critical area. Moreover, all the materials were simulated with homogeneous and isotropic law, despite the dentin and the enamel having an anisotropic behavior in the reality. However, several other studies [49,50] applied the same FEM hypothesis, due to the fact that anisotropy can be observed in a microscopic scale, whereas the tooth is modelled in a macroscopic scale. Lastly,

it should be considered that FEM analysis only considers the mechanical point of view, without considering the biological performance of adhesives, but this is a limitation correlated to the methodology itself.

5. CONCLUSION

This study showed that the FEM can be efficiently used to study interfacial behavior of dental materials in different clinical situations. In particular, all FE meshes, even the restorations, were created starting from micro-CT in order to create realistic dental models. Shear stresses and normal pressure presented similar distributions at the interfaces, and they were influenced in the same way by the different materials considered for the restoration.

Resin composites showed a more homogeneous behavior in stress distribution compared to ceramic. The highly-filled flowable resin composite showed encouraging results when applied as liner, with a significant reduction of shear stresses and normal pressure on the cavity floor and the cervical margin area, especially when the load was applied on an occlusal ceramic material. Cervical enamel margin seemed to play a protective role in the stress distribution, acting as a stress breaker.

Further studies are needed to better assess the influence of shrinkage stress at the interface before loading on the mechanical behavior of different tested materials.

REFERENCES

[1] Veneziani M. Adhesive restorations in the posterior area with subgingival cervical margins: new classification and differentiated treatment approach. Eur J Esthet Dent Off J Eur Acad Esthet Dent 2010;5:50–76.

[2] Cardoso MV, de Almeida Neves A, Mine A, Coutinho E, Van Landuyt K, De Munck J, et al. Current aspects on bonding effectiveness and stability in adhesive dentistry. Aust Dent J 2011;56 Suppl 1:31–44. https://doi.org/10.1111/j.1834-7819.2011.01294.x.

[3] Perdigão J. Dentin bonding as a function of dentin structure. Dent Clin North Am 2002;46:277–301, vi. https://doi.org/10.1016/s0011-8532(01)00008-8.

[4] Kugel G, Ferrari M. The science of bonding: from first to sixth generation. J Am Dent Assoc 1939 2000;131 Suppl:20S-25S. https://doi.org/10.14219/jada.archive.2000.0398.

[5] Van Meerbeek B, Van Landuyt K, De Munck J, Hashimoto M, Peumans M, Lambrechts P, et al. Technique-sensitivity of contemporary adhesives. Dent Mater J 2005;24:1–13. https://doi.org/10.4012/dmj.24.1.

[6] Dietschi D, Scampa U, Campanile G, Holz J. Marginal adaptation and seal of direct and indirect Class II composite resin restorations: an in vitro evaluation. Quintessence Int Berl Ger 1985 1995;26:127–38.

[7] Van Meerbeek B, Perdigão J, Lambrechts P, Vanherle G. The clinical performance of adhesives. J Dent 1998;26:1–20. https://doi.org/10.1016/s0300-5712(96)00070-x.

[8] Ingber JS, Rose LF, Coslet JG. The “biologic width”--a concept in periodontics and restorative dentistry. Alpha Omegan 1977;70:62–5.

[9] Dietschi D, Spreafico R. Current clinical concepts for adhesive cementation of tooth-colored posterior restorations. Pract Periodontics Aesthetic Dent PPAD 1998;10:47–54; quiz 56.

[10] Magne P, Spreafico RC. Deep Margin Elevation: A Paradigm Shift. Am J Esthet Dent 2012;2:11.

[11] Fabianelli A, Sgarr A, Goracci C, Cantoro A, Pollington S, Ferrari M. Microleakage in Class II Restorations: Open vs Closed Centripetal Build-up Technique. Oper Dent 2010;35:308–13. https://doi.org/10.2341/09-128-L.

[12] Baroudi K, Rodrigues JC. Flowable Resin Composites: A Systematic Review and Clinical Considerations. J Clin Diagn Res JCDR 2015;9:ZE18-24. https://doi.org/10.7860/JCDR/2015/12294.6129.

[13] Uçtaşli MB, Bala O, Güllü A. Surface roughness of flowable and packable composite resin materials after finishing with abrasive discs. J Oral Rehabil 2004;31:1197–202. https://doi.org/10.1111/j.1365-2842.2004.01341.x.

[14] Aboushala A, Kugel G, Hurley E. Class II composite resin restorations using glass-ionomer liners: microleakage studies. J Clin Pediatr Dent 1996;21:67–70.

[15] Pereira PNR, Inokoshi S, Tagami J. In vitro secondary caries inhibition around fluoride releasing materials. J Dent 1998;26:505–10. https://doi.org/10.1016/S0300-5712(98)00008-6.

[16] Jokstad A. Secondary caries and microleakage. Dent Mater Off Publ Acad Dent Mater 2016;32:11–25. https://doi.org/10.1016/j.dental.2015.09.006.

[17] Vertolli TJ, Martinsen BD, Hanson CM, Howard RS, Kooistra S, Ye L. Effect of Deep Margin Elevation on CAD/CAM-Fabricated Ceramic Inlays. Oper Dent 2020;45:608–17. https://doi.org/10.2341/18-315-L.

[18] Bresser RA, van de Geer L, Gerdolle D, Schepke U, Cune MS, Gresnigt MMM. Influence of Deep Margin Elevation and preparation design on the fracture strength of indirectly restored molars. J Mech Behav Biomed Mater 2020;110:103950. https://doi.org/10.1016/j.jmbbm.2020.103950.

[19] Juloski J, Köken S, Ferrari M. Cervical margin relocation in indirect adhesive restorations: A literature review. J Prosthodont Res 2018;62:273–80. https://doi.org/10.1016/j.jpor.2017.09.005.

[20] Scotti N, Baldi A, Vergano EA, Tempesta RM, Alovisi M, Pasqualini D, et al. Tridimensional Evaluation of the Interfacial Gap in Deep Cervical Margin Restorations: A Micro-CT Study. Oper Dent 2020. https://doi.org/10.2341/19-161-L.

[21] Jang J-H, Park S-H, Hwang I-N. Polymerization shrinkage and depth of cure of bulk-fill resin composites and highly filled flowable resin. Oper Dent 2015;40:172–80. https://doi.org/10.2341/13-307-L.

[22] Ilie N, Hickel R. Investigations on a methacrylate-based flowable composite based on the SDR™ technology. Dent Mater Off Publ Acad Dent Mater 2011;27:348–55. https://doi.org/10.1016/j.dental.2010.11.014.

[23] Martorelli M, Ausiello P. A novel approach for a complete 3D tooth reconstruction using only 3D crown data. Int J Interact Des Manuf IJIDeM 2013;7:125–33. https://doi.org/10.1007/s12008-012-0166-8.

[24] Magne P. Efficient 3D finite element analysis of dental restorative procedures using micro-CT data. Dent Mater Off Publ Acad Dent Mater 2007;23:539–48. https://doi.org/10.1016/j.dental.2006.03.013.

[25] Versluis A, Tantbirojn D, Pintado MR, DeLong R, Douglas WH. Residual shrinkage stress distributions in molars after composite restoration. Dent Mater Off Publ Acad Dent Mater 2004;20:554–64. https://doi.org/10.1016/j.dental.2003.05.007.

[26] Davidson CL, de Gee AJ. Relaxation of polymerization contraction stresses by flow in

dental composites. J Dent Res 1984;63:146–8. https://doi.org/10.1177/00220345840630021001.

[27] Dejak B, Mlotkowski A. Three-dimensional finite element analysis of strength and adhesion of composite resin versus ceramic inlays in molars. J Prosthet Dent 2008;99:131–40. https://doi.org/10.1016/S0022-3913(08)60029-3.

[28] Ausiello P, Ciaramella S, Fabianelli A, Gloria A, Martorelli M, Lanzotti A, et al. Mechanical behavior of bulk direct composite versus block composite and lithium disilicate indirect Class II restorations by CAD-FEM modeling. Dent Mater Off Publ Acad Dent Mater 2017;33:690–701. https://doi.org/10.1016/j.dental.2017.03.014.

[29] Lawson NC, Bansal R, Burgess JO. Wear, strength, modulus and hardness of CAD/CAM restorative materials. Dent Mater Off Publ Acad Dent Mater 2016;32:e275–83. https://doi.org/10.1016/j.dental.2016.08.222.

[30] Awada A, Nathanson D. Mechanical properties of resin-ceramic CAD/CAM restorative materials. J Prosthet Dent 2015;114:587–93. https://doi.org/10.1016/j.prosdent.2015.04.016.

[31] Zimmerli B, Strub M, Jeger F, Stadler O, Lussi A. Composite materials: composition, properties and clinical applications. A literature review. Schweiz Monatsschrift Zahnmed Rev Mens Suisse Odonto-Stomatol Riv Mens Svizzera Odontol E Stomatol 2010;120:972–86.

[32] Ilie N, Hilton TJ, Heintze SD, Hickel R, Watts DC, Silikas N, et al. Academy of Dental Materials guidance-Resin composites: Part I-Mechanical properties. Dent Mater Off Publ Acad Dent Mater 2017;33:880–94. https://doi.org/10.1016/j.dental.2017.04.013.

[33] Nawafleh N, Hatamleh M, Elshiyab S, Mack F. Lithium Disilicate Restorations Fatigue Testing Parameters: A Systematic Review. J Prosthodont Off J Am Coll Prosthodont 2016;25:116–26. https://doi.org/10.1111/jopr.12376.

[34] Morimoto S, Rebello de Sampaio FBW, Braga MM, Sesma N, Özcan M. Survival Rate of Resin and Ceramic Inlays, Onlays, and Overlays: A Systematic Review and Meta-analysis. J Dent Res 2016;95:985–94. https://doi.org/10.1177/0022034516652848.

[35] D'Arcangelo C, Vanini L, Casinelli M, Frascaria M, De Angelis F, Vadini M, et al. Adhesive Cementation of Indirect Composite Inlays and Onlays: A Literature Review. Compend Contin Educ Dent Jamesburg NJ 1995 2015;36:570–7; quiz 578.

[36] Kielbassa AM, Philipp F. Restoring proximal cavities of molars using the proximal box elevation technique: Systematic review and report of a case. Quintessence Int Berl Ger 1985 2015;46:751–64. https://doi.org/10.3290/j.qi.a34459.

[37] Ausiello P, Apicella A, Davidson CL, Rengo S. 3D-finite element analyses of cusp movements in a human upper premolar, restored with adhesive resin-based composites. J

Biomech 2001;34:1269–77. https://doi.org/10.1016/s0021-9290(01)00098-7.

[38] Chuang S-F, Jin Y-T, Liu J-K, Chang C-H, Shieh D-B. Influence of flowable composite lining thickness on Class II composite restorations. Oper Dent 2004;29:301–8.

[39] Leevailoj C, Cochran MA, Matis BA, Moore BK, Platt JA. Microleakage of posterior packable resin composites with and without flowable liners. Oper Dent 2001;26:302–7.

[40] Meredith N, Sherriff M, Setchell DJ, Swanson SA. Measurement of the microhardness and Young's modulus of human enamel and dentine using an indentation technique. Arch Oral Biol 1996;41:539–45. https://doi.org/10.1016/0003-9969(96)00020-9.

[41] Goel VK, Khera SC, Singh K. Clinical implications of the response of enamel and dentin to masticatory loads. J Prosthet Dent 1990;64:446–54. https://doi.org/10.1016/0022-3913(90)90041-a.

[42] Ausiello P, Franciosa P, Martorelli M, Watts DC. Numerical fatigue 3D-FE modeling of indirect composite-restored posterior teeth. Dent Mater Off Publ Acad Dent Mater 2011;27:423–30. https://doi.org/10.1016/j.dental.2010.12.001.

[43] Magne P, Douglas WH. Design optimization and evolution of bonded ceramics for the anterior dentition: a finite-element analysis. Quintessence Int Berl Ger 1985 1999;30:661–72.

[44] Verdonschot N, Fennis WM, Kuijs RH, Stolk J, Kreulen CM, Creugers NH. Generation of 3-D finite element models of restored human teeth using micro-CT techniques. Int J Prosthodont 2001;14:310–5.

[45] Ausiello P, Ciaramella S, Martorelli M, Lanzotti A, Gloria A, Watts DC. CAD-FE modeling and analysis of class II restorations incorporating resin-composite, glass ionomer and glass ceramic materials. Dent Mater Off Publ Acad Dent Mater 2017;33:1456–65. https://doi.org/10.1016/j.dental.2017.10.010.

[46] van den Breemer CRG, Gresnigt MMM, Cune MS. Cementation of Glass-Ceramic Posterior Restorations: A Systematic Review. BioMed Res Int 2015;2015:1–16. https://doi.org/10.1155/2015/148954.

[47] Zaharia C, Duma V-F, Sinescu C, Socoliuc V, Craciunescu I, Turcu RP, et al. Dental Adhesive Interfaces Reinforced with Magnetic Nanoparticles: Evaluation and Modeling with Micro-CT versus Optical Microscopy. Mater Basel Switz 2020;13. https://doi.org/10.3390/ma13183908.

[48] Sumitani Y, Hamba H, Nakamura K, Sadr A, Nikaido T, Tagami J. Micro-CT assessment of comparative radiopacity of adhesive/composite materials in a cylindrical cavity. Dent Mater J 2018;37:634–41. https://doi.org/10.4012/dmj.2017-310.

[49] Yaman SD, Alaçam T, Yaman Y. Analysis of stress distribution in a maxillary central incisor subjected to various post and core applications. J Endod 1998;24:107–11.

https://doi.org/10.1016/S0099-2399(98)80087-3.

[50] Versluis A, Douglas WH, Cross M, Sakaguchi RL. Does an incremental filling technique reduce polymerization shrinkage stresses? J Dent Res 1996;75:871–8. https://doi.org/10.1177/00220345960750030301.